



Short communication

Pyrolytic carbon from graphite oxide as a negative electrode of sodium-ion battery



Yoshiaki Matsuo*, Koji Ueda

University of Hyogo, 2167 Shosha, Himeji, Hyogo 671-2280, Japan

HIGHLIGHTS

- Pyrolytic carbons with various interlayer spacing were obtained from graphite oxide.
- The reversible capacity reached 252 mAh g⁻¹.
- Sodium ions were inserted between the carbon layers.

ARTICLE INFO

Article history:

Received 24 February 2014

Received in revised form

8 April 2014

Accepted 10 April 2014

Available online 19 April 2014

Keywords:

Sodium-ion battery

Negative electrode

Pyrolytic carbon from graphite oxide

Intercalation

ABSTRACT

Carbons with various interlayer spacings of 0.422–0.334 nm were prepared from the pyrolysis of graphite oxide at various temperatures. Raman measurement indicated that these carbons contain many defects even when the interlayer spacing was almost comparable to that of graphite. The charge and discharge potentials monotonically changed when they were used for the negative electrode of sodium-ion battery, which was rather similar to that observed for soft carbons. The maximum reversible capacity reached 252 mAh g⁻¹ for the carbon prepared at 300 °C and it showed relatively good cycling stability. The X-ray diffraction pattern of it after charged to 0 V indicated that sodium ions are inserted between the carbon layers, forming a stage 1 intercalation compound. The capacity slightly decreased as the increase in the temperature for pyrolysis and more steeply decreased above 900 °C, however, the carbon obtained at 1000 °C still delivered a capacity of 95 mAh g⁻¹.

© 2014 Elsevier B.V. All rights reserved.

1. Introduction

Recently, sodium-ion batteries are attracting much attention as post lithium-ion batteries because the sodium resources are basically unlimited and available everywhere. Sodium insertion materials are used for the electrode materials of sodium-ion battery. For the cathode, sodium containing transition metal oxides such as TiS₂, FeS₂, NaFeO₂, Na_xCoO₂, Na_{2/3}[Ni_{1/3}Mn_{2/3}]O₂, NaNi_{1/2}Mn_{1/2}O₂, etc have been tested [1–7]. On the other hand, for the negative electrode, graphite which is a good host material of lithium ions is not suitable, because the amount of sodium ions intercalated into graphite is very low [8–10]. Therefore, poorly graphitized carbons [11–13], hard carbons [14,15], BC₂N [16], metals, metal oxides or composites of metal and various carbons [17–22] have been tested. Among them, hard carbons which deliver high capacity and show good cycling properties in the presence or absence of additives such

as fluoroethylene carbonate seem promising. However, a large amount of sodium ions are stored in hard carbons at almost 0 V vs Na/Na⁺, which is not favorable to avoid the deposition of sodium metal during cycling from the practical point of view [23].

On the other hand, we have previously reported that lithium ions started to be electrochemically intercalated into pyrolytic carbon from graphite oxide (recently called as graphene oxide) at a high potential of 0.6 V vs Li/Li⁺ and a large amount of lithium ions was stored [24–26]. The interlayer spacings of the carbons were very large, reaching 0.4 nm, though the regularity of the carbon layers was quite high. Interlayer expansion of up to 0.12 nm which was much larger than that observed for graphite (0.04 nm) occurred during lithium insertion. It is expected that a large amount of sodium ions is also intercalated into pyrolytic carbons from graphite oxide. Moreover, when they were prepared at higher temperatures, lithium insertion into them was achieved even in a propylene carbonate based electrolyte solution, though the resulting carbons possessed similar interlayer spacings to that of graphite [27]. These carbons have been known for a long time [28–30] and more recently, they have been extensively investigated from the view

* Corresponding author. Fax: +81 79 267 4898.

E-mail addresses: yamatsuo@eng.u-hyogo.ac.jp, FZJ03774@nifty.com (Y. Matsuo).

points of the preparation of graphene [31–38] or as the electrode materials of electric double layer capacitor [39–41]. To our best knowledge, only one paper on the thermally reduced graphite oxide as a negative electrode of sodium-ion battery has been published [42]. In this case, graphite oxide was first thermally reduced and then was sonicated to exfoliate. The resulting material showed relatively high capacity and good cycling behavior, though it still suffer from a large irreversible capacity. In this paper, the anodic performance of pyrolytic carbons obtained from graphite oxide at various temperatures has been systematically investigated as a negative electrode of sodium-ion battery.

2. Experimental

Graphite oxide was prepared from synthetic graphite powder (Showa Denko Co. Ltd., UF-G30, particle size; 20 μm) in fuming nitric acid using potassium chlorate, based on the Brodie's method [43]. The composition of the resulting GO was $\text{C}_8\text{H}_{2.3}\text{O}_{4.0}$, based on the elemental analysis data of hydrogen (1.51%) and carbon (59.81%). Pyrolysis of GO was performed for 5 h under vacuum at from 300 to 1000 °C with a heating rate of 1 °C min⁻¹ in order to avoid deflagration. Electrochemical performance as a negative electrode of sodium-ion batteries are tested in 0.5 mol dm⁻³ NaClO₄-ethylene carbonate/diethylcarbonate (EC/DEC, 1:1, vol) solution at a constant current 20 mA g⁻¹ under an Ar gas atmosphere using a Hokuto Denko HJ-101SD8 at room temperature. A carbon sample (ca. 5 mg) with polyvinylidene fluoride (PVDF, ca. 0.5 mg) was sandwiched between two Ni mesh current collectors (1 cm²) and pressed at 500 kg cm⁻² for 1 min under a vacuum. It was then dried under a vacuum overnight at 70 °C and was used as a working electrode. The counter and reference electrodes were Na metal. The nitrogen adsorption measurement was performed using Japan Bel, BELSORP max at -196 °C. Raman spectra were recorded using HORIBA Jovin Yvon T-64000 using Ar ion laser with a wavelength of 514.15 nm. X-ray diffraction patterns were obtained using Rigaku RINT-2100 and Si powder (Soekawa Chem, 4 μm) was used as an internal reference. The diffraction angle was corrected based on that of the (111) peak of Si added as an internal standard.

3. Results and discussion

3.1. Preparation and characterization of carbons from the pyrolysis of GO

Fig. 1 shows the X-ray diffraction patterns of graphite oxide before and after heated at various temperatures. The diffraction

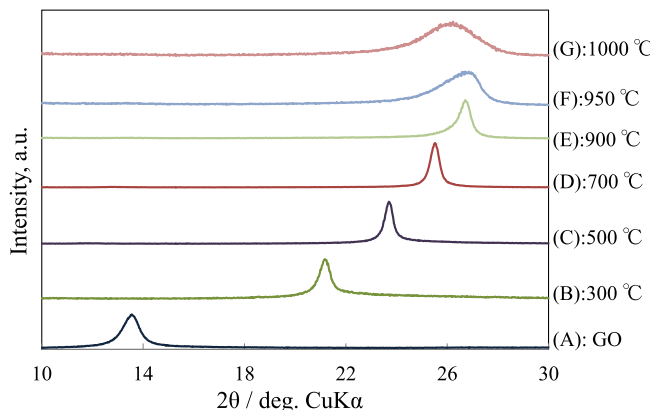


Fig. 1. X-ray diffraction patterns of (A): GO and those pyrolyzed at (B): 300, (C): 500, (D): 700, (E): 900, (F): 950 and (G): 1000 °C.

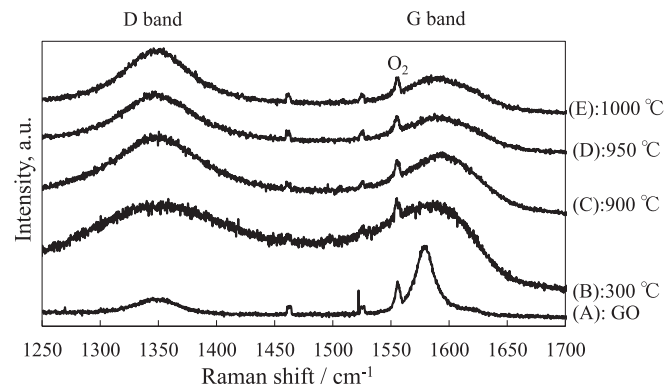


Fig. 2. Raman spectra of (A): GO and those pyrolyzed at (B): 300, (C): 900 and (D): 950 °C.

peak at $2\theta = 14.4^\circ$ observed for GO shifted to higher angle of $2\theta = 21.04^\circ$ after heated 300 °C. It further shifted to higher angle and reached $2\theta = 26.56^\circ$ at 900 °C. The interlayer spacing decreased from 0.422 to 0.334 nm as was observed for the pyrolytic carbon prepared from GO under hydrogen gas flow [26]. When the temperature reached at 1000 °C, the diffraction peak shifted to a lower angle of $2\theta = 26.5^\circ$ and the interlayer spacing slightly increased to 0.339 nm. The decrease of the interlayer spacing is ascribed to the removal of oxygen functional groups bonded to carbon layers of GO. The reason why the interlayer spacing became smaller than that of graphite (0.3354 nm) is not clear at this moment, however, the loss of carbon atoms from the carbon layers together with oxygen functionalities could be related to this unusually small interlayer spacing. In order to reconstruct six membered rings, reorientation of carbon atoms within the carbon layers should be needed, which may cause the increase in the interlayer spacing at a higher temperature of 1000 °C. Introduction of strain on the carbon layers as the result of removal of carbon atoms in them has been suggested, based on the theoretical calculation [44]. Fig. 2 shows the Raman spectra of GO and PGO samples obtained at various temperatures. The D and G bands were observed at 1330 and 1583 cm⁻¹ for pristine GO and these peaks slightly shifted to higher wavenumber of 1338 and 1583 cm⁻¹ after pyrolysis, respectively. The shape of the spectra of PGO samples was almost identical for those obtained even at 900 °C, though their interlayer spacings of them were almost the same as that of graphite. The large intensity ratios of D and G bands indicate that these samples still contained a large number of defects.

Fig. 3 shows the nitrogen adsorption isotherms for PGO300, PGO900 and PGO950. The isotherms of PGO300 and PGO900 were

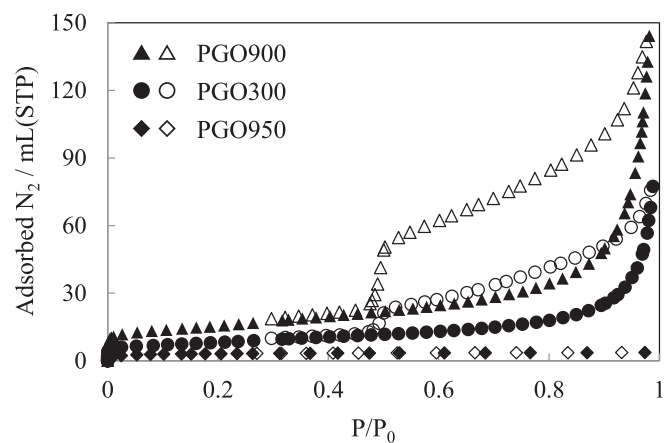


Fig. 3. Adsorption isotherms of GO pyrolyzed at 300, 900 and 950 °C.

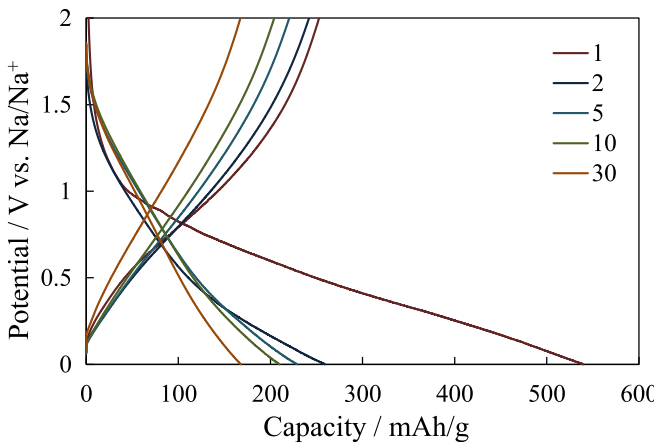


Fig. 4. Charge discharge curves of PGO300 in 0.5 M NaClO_4 -EC/DEC.

type IV, indicating that they contain mesopores. The BET surface area increased from 29 to $54 \text{ m}^2 \text{ g}^{-1}$, as the increase in the temperature for pyrolysis. The isotherm of PGO950 changed to type I and the adsorbed amount of nitrogen greatly decreased. The BET surface area was only $2.6 \text{ m}^2 \text{ g}^{-1}$.

3.2. Anodic performance of carbons from the pyrolysis of GO

Fig. 4 shows the charge–discharge curves of carbons obtained from the pyrolysis of GO at 300°C in 0.5 M NaClO_4 -EC/DEC (1:1) electrolyte solution. During charging, the potential sharply decreased to 1.5 V and then monotonously decreased to 0 V and the charge capacity reached 540 mAh g^{-1} . During discharging, it increased almost linearly until it reached 1.2 V and then increased more steeply. The first discharge capacity was 252 mAh g^{-1} . This value is almost comparable to that reported to some hard carbons [14]. In the second cycle, the potential gradually decreased from 0.9 V and the discharge curve was similar to that observed in the first cycle. As shown in **Fig. 5**, the capacity gradually decreased during cycling, however, PGO300 still delivered 170 mAh g^{-1} even after 30 cycles which was 66% of that of the first cycle. The shape of the charge curve of the present sample is not favorable from the view point of the energy density, however, is advantageous to avoid the deposition of sodium metals during cycling. The coulombic efficiency of the first cycle was very low, ca.50%, however, it approached 100% in the subsequent cycles. This suggests that the irreversible capacity at the first cycle was mostly ascribed to the decomposition of electrolyte and the formation of SEI film.

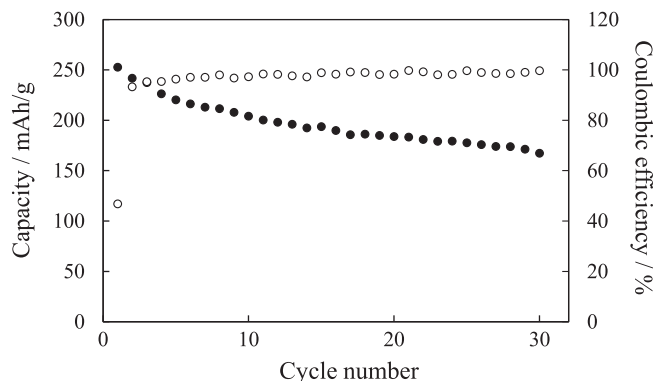


Fig. 5. Cycling properties (filled circles) and coulombic efficiency (open circles) of PGO300.

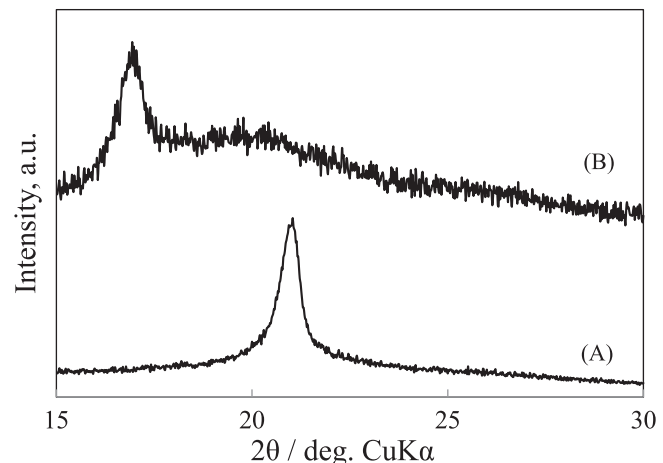


Fig. 6. X-ray diffraction patterns of PGO300 (A): before and (B): after charged to 0 V.

Considering the lower cycling efficiency observed for highly exfoliated PGO samples prepared from natural graphite powder (not shown), the irreversible capacity after 2nd cycle could be mainly due to the loss of electrical contact of the PGO particles. The insertion/extraction of sodium ions into/from PGO seems reversible.

Fig. 6 shows the X-ray diffraction patterns of PGO300 after charged to 0 V during the first cycle. The diffraction peak observed at $2\theta = 21.04^\circ$ ($d = 0.422 \text{ nm}$) before discharge greatly shifted to $2\theta = 16.94^\circ$ (0.523 nm) after charged to 0 V. The increase in the interlayer spacing of 0.101 nm was very similar to that observed for sodium intercalated graphite of 0.117 nm (0.452 nm – 0.335 nm) [8–10], therefore, sodium ions are stored between the layers of PGO300, forming stage 1 intercalation compound. It has been reported that sodium ions were more easily intercalated into carbon or carbon based materials in the following conditions. The first one is the presence of impurities such as hydrogen, nitrogen, oxygen, etc [45]. The lowering of the Fermi level is the other factor to facilitate the intercalation of sodium ions, which was observed for the intercalation into soft carbons [46]. Kawaguchi et al. indicated that the absorption due to unoccupied π^* orbital of BC_2N into which a considerable amount of sodium ions was intercalated was relatively strong in its intensity, and the bottom of the π^* orbital was lower in energy than each bottom of HOPG or noncrystalline carbon, based on the X-ray absorption spectroscopy [15]. In case of the present PGO300, it still contained 0.15 and 17.3% of hydrogen and oxygen, based on the elemental analysis. Moreover, a number of synchrotron X-ray absorption and emission analyses of thermally reduced GO have been recently reported and they indicate that the Fermi level and the DOS of it is rather similar to those of graphite [37,47]. This suggests that the electronic structure of PGO is more similar to that of graphite than BC_2N in terms of the Fermi level and the DOS in unoccupied π^* orbital. Therefore, the impurities in PGO300 would be the main factor to facilitate the intercalation of sodium ions into it.

Fig. 7 shows the 1st charge and discharge curves of carbons obtained from the pyrolysis of GO at various temperatures, together with that of graphite. The potential during charging decreased as the increase in the temperature for pyrolysis and a plateau at 0.6 V due to the SEI formation more clearly appeared for the samples prepared 700°C or higher. The decrease in the content of oxygen containing functional groups remaining in PGO samples which are reduced at a higher potentials would result in this change of the shape of the charge curves. The charge capacity decreased with the increase in the temperature for pyrolysis and became 250 mAh g^{-1}

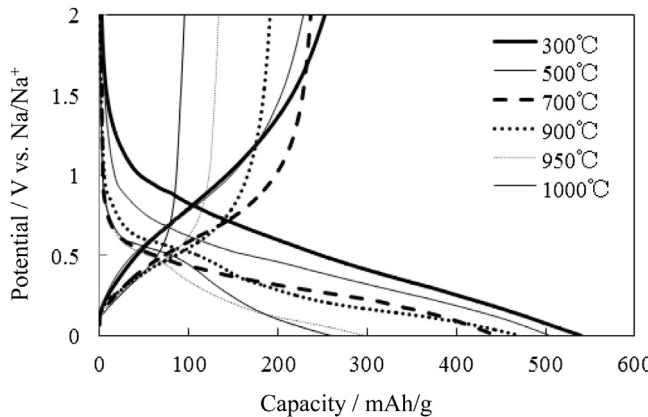


Fig. 7. Charge–discharge curves of GO pyrolyzed at 300, 500, 700, 900, 950 and 1000 °C, together with that of graphite.

for PGO1000. The potential during discharging started to increase at 0.1 V for all the samples. The discharge potential of PGO500 changed in a similar manner to that of PGO300. The discharge potential of the samples obtained at 700 °C or higher increased monotonically in almost the same manner at the beginning, however, it started to increase steeply at lower potentials as the temperature for pyrolysis became higher. Accordingly, the discharge capacity became smaller for the samples obtained at higher temperatures. Fig. 8 shows the relationship between charge and discharge capacities of PGO samples as a function of temperature for pyrolysis. Both slightly decreased with the increase in the temperature and then steeply decreased above 900 °C. The decrease in the remaining oxygen and hydrogen as impurities in PGO would reduce the amount of stored sodium ions in PGO samples obtained at higher temperatures. On the other hand, the decrease in the charge capacity for these samples could be ascribed to that in the surface area. It is very interesting that much higher amounts of sodium ions were still stored in carbons with similar interlayer spacings (PGO900, PGO950 and PGO1000) to that of graphite in which very few amounts of sodium ions are stored.

4. Conclusions

Pyrolytic carbons from graphite oxide were prepared at various temperatures. The interlayer spacing varied between 0.334 and 0.422 nm. The potential of these carbons almost monotonically

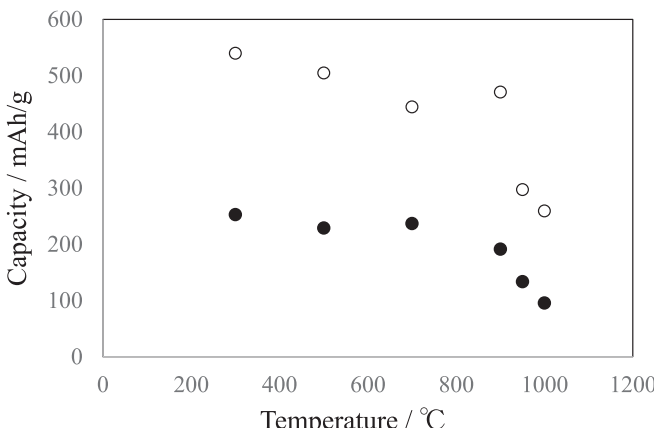


Fig. 8. Variation of charge and discharge capacities of PGO samples as a function of temperature for pyrolysis.

changed during charging, which was different from that observed for hard carbons in which a large amount of sodium ions are stored in nanopores around 0 V vs. Na/Na⁺ [48]. The X-ray diffraction pattern of PGO300 charged to 0 V indicated that sodium ions are stored between the carbon layers of PGO300, forming a stage 1 intercalation compound. This behavior would be favorable in order to avoid the deposition of sodium metal during cycling. The maximum reversible capacity of 252 mAh g⁻¹ was obtained for the carbon prepared at 300 °C and it showed relatively good cycling stability. The capacity slightly decreased as the increase in the temperature for pyrolysis and more steeply decreased above 900 °C. However, the carbon obtained at 1000 °C still delivered a capacity of 95 mAh g⁻¹, which was much larger than that observed for graphite. The low 1st coulombic efficiency should be improved, however, pyrolytic carbons from graphite oxide would be promising for the negative electrode of sodium ion battery.

References

- [1] M.S. Whittingham, Prog. Solid State. Chem. 12 (1978) 41–99.
- [2] Y. Takeda, K. Nakahara, M. Nishijima, N. Imanishi, O. Yamamoto, M. Takano, R. Kanno, Mat. Res. Bull. 29 (1994) 659–666.
- [3] M. Tsuda, H. Arai, M. Takahashi, H. Ohtsuka, Y. Sakurai, K. Sumitomo, H. Kageshima, J. Power Sources 144 (2005) 183–190.
- [4] N. Yabuuchi, H. Yoshida, S. Komaba, Electrochemistry 80 (2012) 716–719.
- [5] S. Komaba, N. Yabuuchi, T. Nakayama, A. Ogata, T. Ishikawa, I. Nakai, Inorg. Chem. 51 (2012) 6211–6622.
- [6] N. Yabuuchi, M. Kajiyama, J. Iwatake, H. Nishikawa, S. Hitomi, R. Okuyama, R. Usui, Y. Yamada, S. Komaba, Nat. Mater. 11 (2012) 512–517.
- [7] Y. Kawabe, N. Yabuuchi, M. Kajiyama, N. Fukuura, T. Inamasu, R. Okuyama, I. Nakai, S. Komaba, Electrochim. Commun. 13 (2011) 1225–1228.
- [8] R.C. Asher, J. Inorg. Nucl. Chem. 10 (1959) 238–249.
- [9] A. Metrot, A. Hérolé, J. Chim. Phys. (1969) 71–79.
- [10] A. Metrot, D. Guérard, D. Billaud, A. Hérolé, Synth. Met. 1 (1980) 363–369.
- [11] D.A. Stevensa, J.R. Dahn, J. Electrochim. Soc. 147 (2000) 1271–1273.
- [12] R. Alcántara, J.M. Jiménez-Mateos, P. Lavela, J.L. Tirado, Electrochim. Commun. 3 (2001) 639–642.
- [13] R. Alcántara, J.M. Jiménez-Mateos, J.L. Tirado, J. Electrochim. Soc. 149 (2002) A201–A205.
- [14] S. Komaba, W. Murata, T. Ishikawa, N. Yabuuchi, T. Ozeki, T. Nakayama, A. Ogata, K. Gotoh, K. Fujiwara, Adv. Funct. Mater. 21 (2011) 3859–3867.
- [15] A. Ponrouch, A.R. Goñia, M. Rosa Palacín, Electrochim. Commun. 27 (2013) 85–88.
- [16] M. Kawaguchi, K. Ohnishi, K. Yamada, Y. Muramatsu, J. Electrochim. Soc. 157 (2010) P13–P17.
- [17] M.C. López, P. Lavela, G.F. Ortiz, J.L. Tirado, Electrochim. Commun. 27 (2013) 152–155.
- [18] Q. Sun, Q.-Q. Ren, H. Li, Z.-W. Fu, Electrochim. Commun. 13 (2011) 1462–1464.
- [19] L. Baggetto, E. Allcorn, A. Manthiram, G.M. Veith, Electrochim. Commun. 27 (2013) 168–171.
- [20] M.K. Datta, R. Epur, P. Saha, K. Kadakia, S.K. Park, P.N. Kumta, J. Power Sources 225 (2013) 316–322.
- [21] L. Wu, F. Pei, R. Mao, F. Wu, Y. Wu, J. Qian, Y. Cao, X. Ai, H. Yang, Electrochim. Acta 87 (2013) 41–45.
- [22] D. Su, H.-J. Ahn, G. Wang, Chem. Commun. 49 (2013) 3131–3133.
- [23] Y. Sun, L. Zhao, H. Pan, X. Lu, L. Gu, Y.-S. Hu, H. Li, M. Armand, Y. Ikuhara, L. Chen, X. Huang, Nat. Commun. 4 (2013) 1870.
- [24] Y. Matsuo, Y. Sugie, Carbon 36 (1998) 301–303.
- [25] Y. Matsuo, Y. Sugie, Denki Kagaku 66 (1998) 1288–1290.
- [26] Y. Matsuo, Y. Sugie, J. Electrochim. Soc. 146 (1999) 2011–2014.
- [27] Y. Matsuo, Y. Sugie, Electrochim. Solid-State Lett. 1 (1998) 204–206.
- [28] V. Kohlschütter, P. Haenni, Z. Anorg. Chem. 105 (1919) 121–144.
- [29] R.J. Beekett, R.C. Croft, J. Phys. Chem. 56 (1952) 929–935.
- [30] E. Matuyama, J. Phys. Chem. 58 (1954) 215–219.
- [31] M. Acik, G. Lee, C. Mattevi, A. Pirkle, R.M. Wallace, M. Chhowalla, K. Cho, Y. Chabal, J. Phys. Chem. C 115 (2011) 19761–19781.
- [32] A. Bagri, C. Mattevi, M. Acik, Y.J. Chabal, M. Chhowalla, V.B. Shenoy, Nat. Chem. 2 (2010) 581–587.
- [33] D. Yan, A. Velamakanni, G. Bozoklu, S. Park, M. Stoller, R.D. Piner, S. Stankovich, I. Jung, D.A. Field, C.A.J. Ventrice, R.S. Ruoff, Carbon 47 (2009) 145–152.
- [34] O. Akhavan, Carbon 48 (2010) 509–519.
- [35] C. Mattevi, G. Eda, S. Agnoli, S. Miller, K.A. Mkhoyan, O. Celik, D. Mastrogiovanni, G. Granozzi, E. Garfunkel, M. Chhowalla, Adv. Funct. Mater. 19 (2009) 2577–2583.
- [36] R. Larciprete, S. Fabris, T. Sun, P. Lacovig, A. Baraldi, S. Lizzit, J. Am. Chem. Soc. 133 (2011) 17315–17321.

- [37] A. Ganguly, S. Sharma, P. Papakonstantinou, J. Hamilton, *J. Phys. Chem. C* 115 (2011) 17009–17019.
- [38] M. Acik, C. Mattevi, C. Gong, G. Lee, K. Cho, M. Chhowalla, Y. Chabal, *ACS Nano* 4 (2010) 5861–5868.
- [39] M.M. Hantel, T. Kaspar, R. Nesper, A. Wokaun, R. Kötz, *Electrochem. Commun.* 13 (2011) 90–92.
- [40] M.M. Hantel, T. Kaspar, R. Nesper, A. Wokaun, R. Kötz, *Chem. Eur. J.* 18 (2012) 9125–9136.
- [41] H.D. Yoo, Y. Park, J.H. Ryu, S.M. Oh, *Electrochim. Acta* 56 (2011) 9931–9936.
- [42] Y.-X. Wang, S.-L. Chou, H.-K. Liu, S.-X. Dou, *Carbon* 57 (2013) 202–208.
- [43] M.B.C. Brodie, *Ann. Chim. Phys.* 59 (1860) 466–472.
- [44] H.C. Schiepp, J.Lu Li, M.J. McAllister, H. Sai, M. Herrera-Alonso, D.H. Adamson, R.K. Rrud'homme, R. Car, D.A. Saville, I.A. Aksay, *J. Phys. Chem. B* 110 (2006) 8535–8539.
- [45] M. El Gadi, A. Hérolde, C. Hérolde, P. Lagrange, M. Lelaurain, J.F. Maréchié, *Mol. Cryst. Liq. Cryst.* 244 (1994) 29–34.
- [46] M.C. Robert-Picard, M. Oberlin, J. Mering, C. R. Acad. Sci. Ser. C 266 (1968) 1043–1045.
- [47] V. Lee, R.V. Dennis, B.J. Schultz, C. Jaye, D.A. Fischer, S. Banerjee, *J. Phys. Chem. C* 116 (2012) 20591–20599.
- [48] K. Gotoh, T. Ishikawa, S. Shimadzu, N. Yabuuchi, S. Komaba, K. Takeda, A. Goto, K. Deguchi, S. Ohki, K. Hashi, T. Shimizu, H. Ishida, *J. Power Sources* 225 (2013) 137–140.